3051-1-T = RL-2092

THE UNIVERSITY OF MICHIGAN

COLLEGE OF ENGINEERING

DEPARTMENT OF ELECTRICAL ENGINEERING

Radiation Laboratory

VOR PARASITIC LOOP COUNTERPOISE SYSTEMS-II

Interim Report No. 1 (27 June - 31 October 1969

By

Dipak L. Sengupta and Joseph E. Ferris

15 November 1969

Contract FA 69 WA-2085, Project 330-001-03N
Contract Monitor: Mr. Sterling Anderson

CONTRACT WITH

Federal Aviation Administration
Radar and Navaids Section
800 Independence Avenue, SW
Washington, DC 20590

Ann Arbor, Michigan

1. Introduction

This is the First Interim Report on Contract FA 69-WA-2085, Project 330-001-03N "VOR Parasitic Loop Counterpoise Systems-II" and covers the period 27 June to 31 October 1969

During this period we have carried out theoretical and experimental investigations of the radiation characteristics of parasitic loop counterpoise antennas over the frequency range 1.000 - 1.200 GHz. The counterpoise diameter used was 15' so that it corresponds to the actual 150' diameter counterpoise at the full scale frequency. Theoretical results reported herein pertain to the case when the excited element produces omnidirectional patterns in the azimuthal plane. Experimental results have been obtained for both omnidirectional and figure-of-eight types of excitation. The experimental results obtained in the latter case should be regarded as preliminary and hence are not complete. In the following sections we discuss very briefly some of the results obtained so far. Detailed critical discussions of all the results will be reported in our future reports.

2. Omnidirectional Excitation

In this section we discuss the radiation pattern characteristics of the parasitic loop counterpoise antenna when the excited element above the counterpoise has an omnidirectional free-space pattern in azimuth, i.e. the antenna uses a single Alford loop as the feed element. The tenth scale Alford loop model is located axially at a height 4.8" above the 15' diameter counterpoise. The design and construction of the Alford loop have been discussed elsewhere (Sengupta, et al, 1968)[+] and will not be repeated here.

2.1 Alford Loop Counterpoise Radiation Pattern

The measured free space far field elevation pattern of the Alford loop above the 15' diameter counterpoise is shown in Fig. 1. The theoretical pattern of the same antenna, obtained by numerically computing the far field expression (Sengupta et al, 1968)[+], is superposed on Fig. 1 for comparison. The agreement between theory and experiment may be considered to be excellent over most of the regions in space. The slight kink in the experimental pattern near the region $\theta = 95^{o}$ is attributed to a reflecting object lying near the outside pattern range. Theoretical values of the important parameters

---

[+] Sengupta, D. L., J. E. Ferris and V. H. Weston (September 1968), "Theoretical and Experimental Investigation of Parasitic Loop Counterpoise Antennas," SRDS Report RD-68-50, The University of Michigan Radiation Laboratory Report 8905-1-F, Contract FA 67-WA-1753.

characterizing the free-space elevation pattern of the Alford loop above a 15' diameter counterpoise are given below.

Direction of principal maximum $\theta_{max} = 65^o$

Far field gradient at the horizon $\alpha_g = 5.56$ dB/6^o

Field reduction factor $\alpha_F = -20 \log_{10} \left| \frac{E(90^o)}{E(\theta_{max})} \right| = 14.85$ dB .

The omnidirectionality of the pattern in the azimuthal plane has been found to be good in most of the regions in space.

2.2 Single Parasitic Loop Counterpoise Antenna Radiation Pattern

The present section discusses the far field elevation pattern obtained when a parasitic loop of suitable diameter is placed coaxially above and parallel to the basic Alford loop counterpoise antenna discussed in the previous section. From a study of the numerical results it appeared that a parasitic loop having a radius B such that $kB = 3\pi$ (i.e. $2B = 3\lambda$) would produce a good field gradient when placed at a proper height H above the counterpoise. The parasitic loop was made of 1-inch wide conducting strip. The theoretical field gradient as a function of the height H of the parasitic loop above the counterpoise is shown in Fig. 2. It can be seen from Fig. 2 that such a parasitic loop counterpoise antenna having $kH = 13$ and $kB = 3\pi$ produces a maximum field gradient of 9.6 dB/6^o. The complete theoretical far field elevation pattern of such an antenna is shown in Fig. 3. The measured far field elevation pattern of a single parasitic loop counterpoise antenna is shown in Fig. 4(a) and 4(b). The detailed comparison between experiment and theory for this case will be carried out later but the agreement appears to be good for the results presented here. The field gradient obtained from the pattern shown in Fig. 4 is found to be better than 16 dB/6^o.

2.3 Double Parasitic Loop Counterpoise Radiation Pattern

So far only numerical results have been obtained for the radiation patterns of double parasitic loop counterpoise antennas. On the basis of numerical results obtained so far it has been found that a double parasitic loop counterpoise antenna with $kB_1 = 4\pi$, $kH_1 = 3.75$, $kB_2 = 10.68$ and $kH_2 = 13.1$ produces a field gradient $\alpha_g = 14.8$ dB/6^o. The parameters of this antenna have not been optimized for best field gradient. It is anticipated that after they are optimized the field gradient would be much better. Theoretical optimization of the antenna as well as the results of its pattern measurements will be reported in the future.

2.4 Numerical Results on Parasitic Current

A computer program has been developed for obtaining the current induced in the parasitic loop when the excitation is omnidirectional. Detailed discussions of the theoretical expressions for the current induced in the parasitic loop have been given in the final report on the previous study (8905-1-F, RD-68-50, Sept. 68). Here we only quote the final expressions without derivation. The normalized induced current in the parasitic loop can be written in the following form:

$$\frac{I_{p_o}}{I_o} = I_{p_o}^{12} + I_{p_o}^{34} + I_{p_o}^{56} \quad , \tag{1}$$

where I_{p_o}/I_o is the current in the parasitic loop normalized with respect to the current in the Alford loop. The right-hand side of Eq. (1) is split into three terms for theoretical reasons explained in the reference (8905-1-F, RD-68-50, Sept. '68). It can be shown that the three terms on the right-hand side of (1) are given by

$$I_{p_o}^{12} = \frac{2\pi B}{ikM}\left[\frac{e^{ikr_1}}{r_1^2} - \frac{e^{ikr_2}}{r_2^2}\right] \quad , \tag{2}$$

$$\left.\begin{aligned} r_1^2 &= B^2+(H-h)^2, \quad r_2^2 = B^2+(H+h)^2 \\ M &= 0.577 + \ell n\,(kb/2) - i\pi/2 \end{aligned}\right\} \tag{3}$$

$$I_{p_o}^{34} = \frac{\pi}{ikM}\,\frac{A}{r_o^2}\,e^{ikr_o}\,\frac{e^{-i3\pi/4}}{\sqrt{2}}\,\left(\frac{A}{B}\right)^{1/2} \times$$

$$\times\left[\left(\frac{1}{\pi kr_3}\right)^{1/2} e^{ikr_3}\left\{\sec\left(\frac{\phi_o-\phi_3}{2}\right) - \sec\left(\frac{\phi_o+\phi_3}{2}\right)\right\}\right.$$

$$\left. + i\left(\frac{1}{\pi kr_4}\right)^{1/2} e^{ikr_4}\left\{\sec\left(\frac{\phi_o-\phi_4}{2}\right) - \sec\left(\frac{\phi_o+\phi_4}{2}\right)\right\}\right] , \tag{4}$$

$$\left.\begin{aligned} r_3^2 &= (A-B)^2+H^2; \quad r_4^2 = (A+B)^2+H^2 \\ r_o^2 &= A^2+h^2 \\ \tan\phi_3 &= \frac{H}{A-B}\ , \quad \tan\phi_4 = \frac{H}{A+B}, \quad \tan\phi_o = \frac{h}{A} \end{aligned}\right\} \tag{5}$$

$$I_{p_o}^{56} = \frac{\pi^2 (kB)}{M^2} \frac{e^{ikr_1}}{(kr_1)^2} \left[\left(\frac{1}{\pi kB}\right)^{1/2} e^{i(2kB+\pi/4)} - \left(\frac{1}{\pi kH}\right)^{1/2} e^{i(2kH-\pi/4)} \right]. \quad (6)$$

The various notations used in Eqs. (2) - (6) are as explained in the reference cited (8905-1-F, RD-68-50, Sept. '68). Numerical values for the parasitic current have been obtained for a typical single parasitic loop counterpoise antenna having the following parameters: kA=17.92, kb=0.15, kh=2.75, kB=3π, kH=11.78. The values obtained for the normalized current are shown in the table below.

	Real	Imaginary	Absolute Value	Argument Radians
$I_{p_o}^{12}$	-0.03893	0.17908	0.18326	1.785
$I_{p_o}^{34}$	-0.00070	0.00035	0.00078	2.678
$I_{p_o}^{56}$	0.02911	-0.00159	0.02915	-0.055
$\frac{I_{p_o}}{I_o}$	-0.01052	0.17784	0.17815	1.630

Parasitic currents induced for other cases will be computed in the future and the results will be discussed in our future report.

2.5 Mutual Coupling Effects

For double parasitic loop counterpoise antennas the effects of mutual coupling between the parasitic loops appear to be quite important for the calculation of induced currents as well as the far field pattern of the complete antenna. The above computer problem for the evaluation of the current will be modified in the future so that the mutual coupling effects can be taken into account. Similar modification of the computer program would be needed to obtain the theoretical far field patterns of double parasitic loop counterpoise antennas.

3. Figure-of-Eight Excitation

Only experimental results have been obtained with this type of excitation.

3.1 Excited Element Pattern

The excited element here consists of two similar Alford loops fed 180^{o} out of phase and placed in the same plane which is parallel to the counterpoise. The two loops are placed at a height of 4.8" above the counterpoise . They are displaced on either side of the axis of the counterpoise by 1.6" so that the two Alford loops are 3.2" apart. Figure 5 shows a photograph of the double Alford loop counterpoise model used during the experiment. The far field patterns produced by this antenna have been measured over the frequency range 1.0 - 1.2 GHz. Typical patterns obtained at the frequency 1.080 GHz are shown in Figs.6(a) and 6(b). Notice that the ground plane used for this test has a diameter of 22" .

3.2 Single Parasitic Loop Case

A single parasitic loop counterpoise has been fabricated with the above exciter along with a 15' diameter counterpoise. The far field pattern produced by such an antenna has been measured and a typical pattern is given in Fig. 7. It can be seen from this figure that a lobe appears in the axial direction ($\theta=0^{o}$). This is attributed to the non-uniform excitation of the parasitic loop. However, it is anticipated that with a proper choice of height H of the parasitic loop it would be possible to reduce this lobe considerably by utilizing the concept of image. The result presented in Fig.7 does show some improvement in the field gradient (7.5 dB/6^{o}). However, the field gradient may be improved more by choosing the proper diameter of the parasitic loop. Work along this line will be carried out during the next period.

4. Conclusions

The above results represent the present status of the numerical and experimental investigation of the radiation characteristics of the VOR parasitic loop counterpoise antenna system with omnidirectional and figure-of-eight types of excitation in the azimuthal plane. The investigation of single parasitic loop counterpoise antennas with omnidirectional excitation has been completed. The double parasitic loop case with similar excitation will be optimized in the future for best field gradient. More study is necessary to determine the effectiveness of using parasitic loops when the excitation used is of the figure-of-eight type. It is recommended that more theoretical studies be carried out to take into account the effects of mutual coupling on the induced currents as well as the radiation fields of double parasitic loop counterpoise antennas.

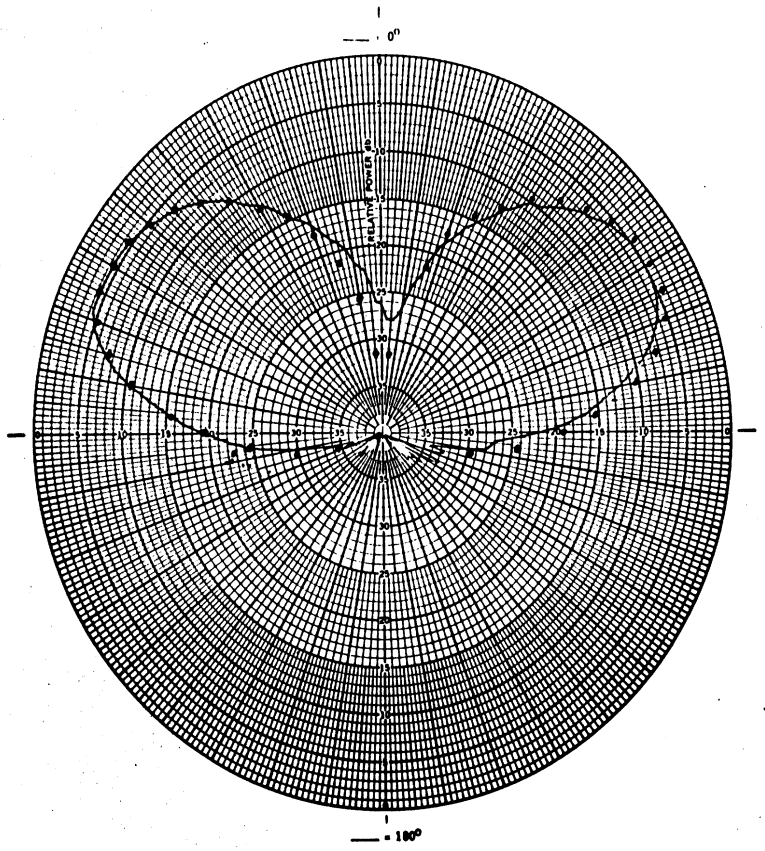

FIG. 1: Far Field Elevation Pattern of Alford Loop Counterpoise Antenna. kh=2.75, kA=51.69, f=1080 MHz
—— Measured, • • • Theoretical.

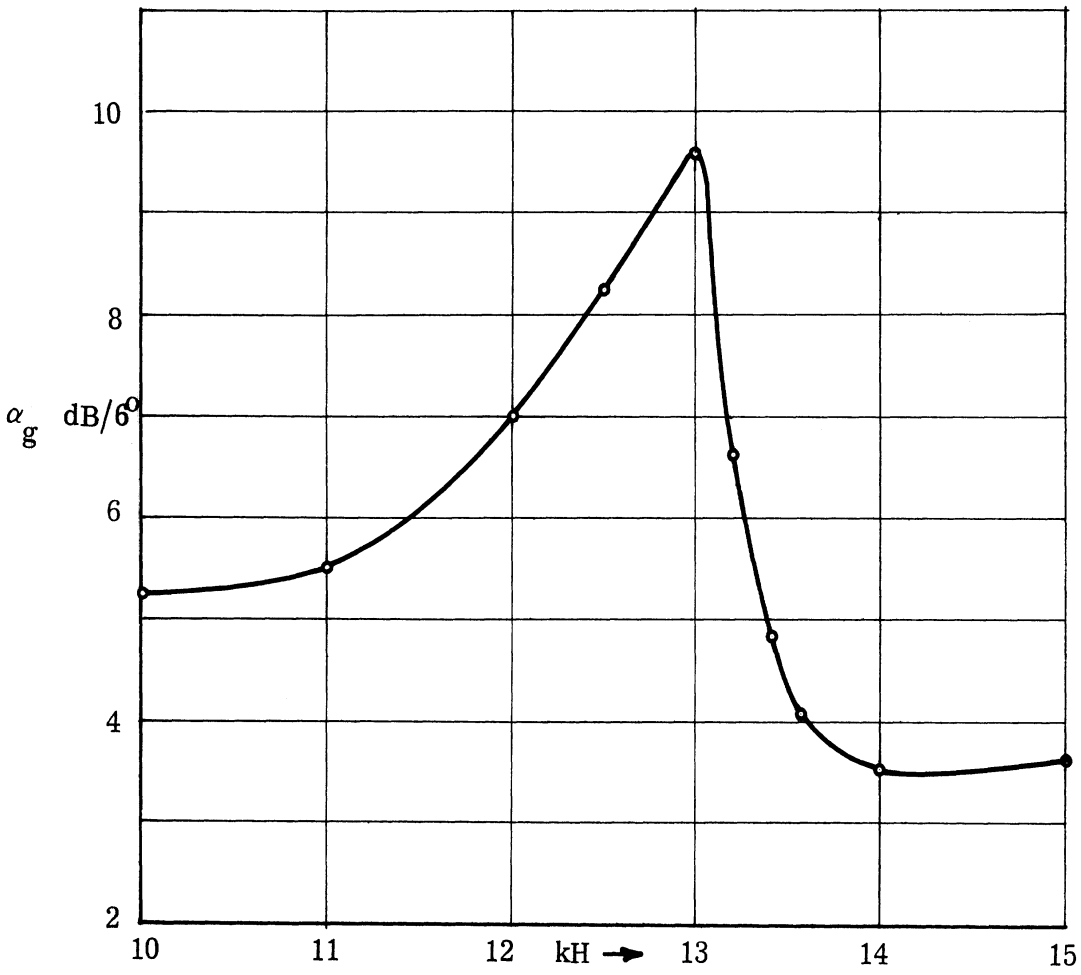

FIG. 2: Theoretical Field Gradient (α_g) as a function of H for a Single Parasitic Loop Counterpoise Antenna. kh=2.75, kA=51.69, kB= 3π, kH variable.

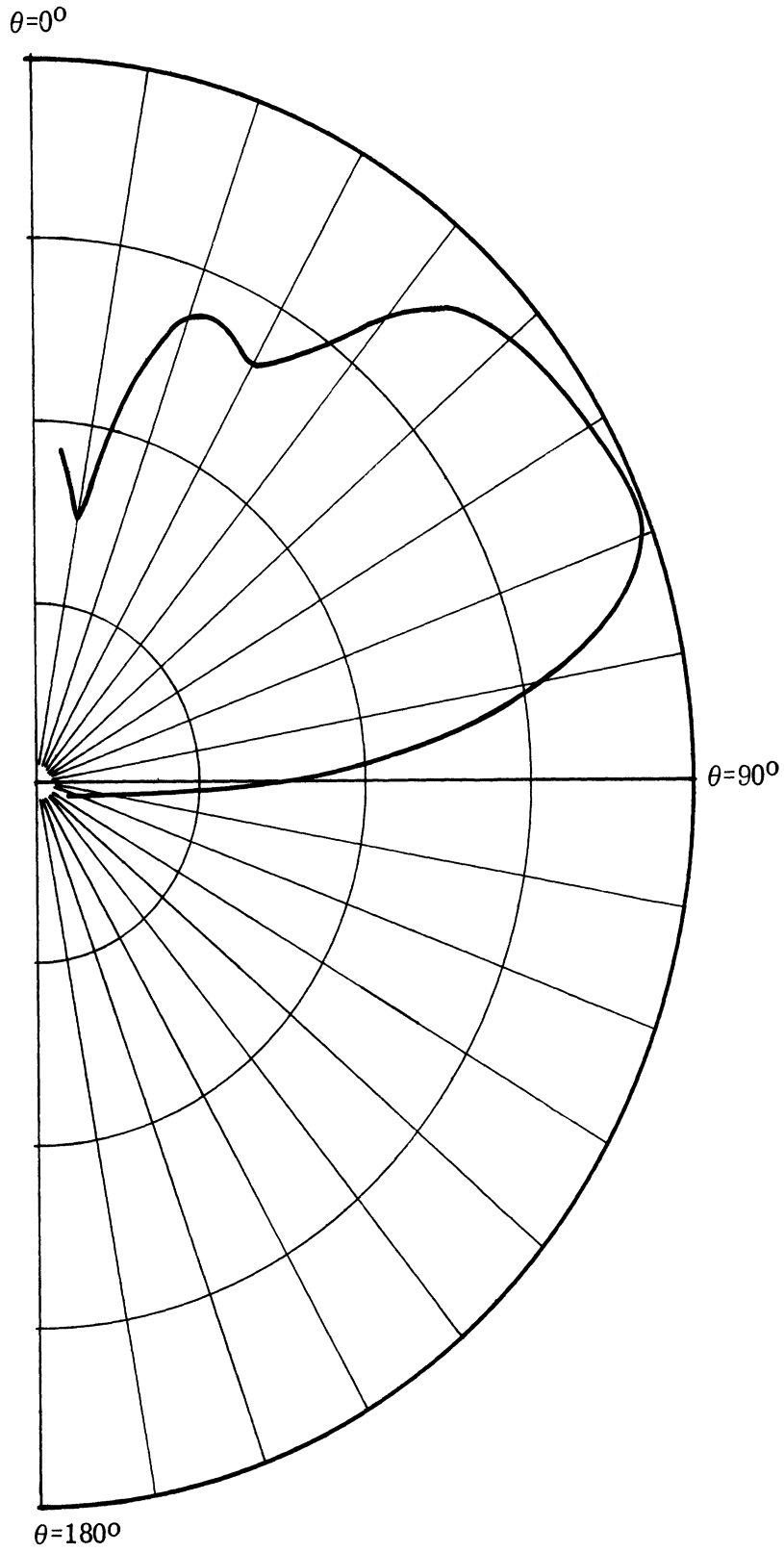

FIG. 3: Theoretical Far Field Elevation Pattern of a Single Parasitic Loop Counterpoise Antenna. kh=2.75, kA=51.69, kH=13, kB= 3π, f = 1080 MHz.

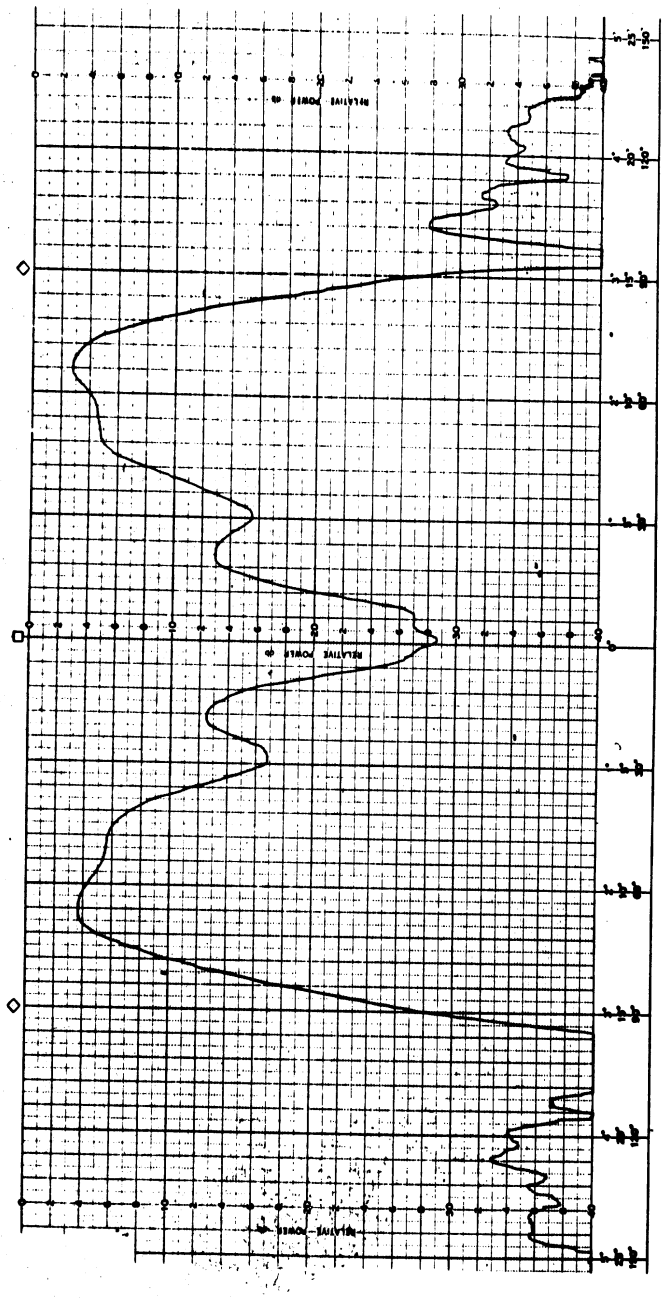

FIG. 4(a): Measured Far Field Elevation Pattern of a Single Parasitic Loop Counterpoise Antenna - Complete Pattern. h=4.8", 2A=15', H=22.5", 2B=31.75" and f = 1080 MHz.

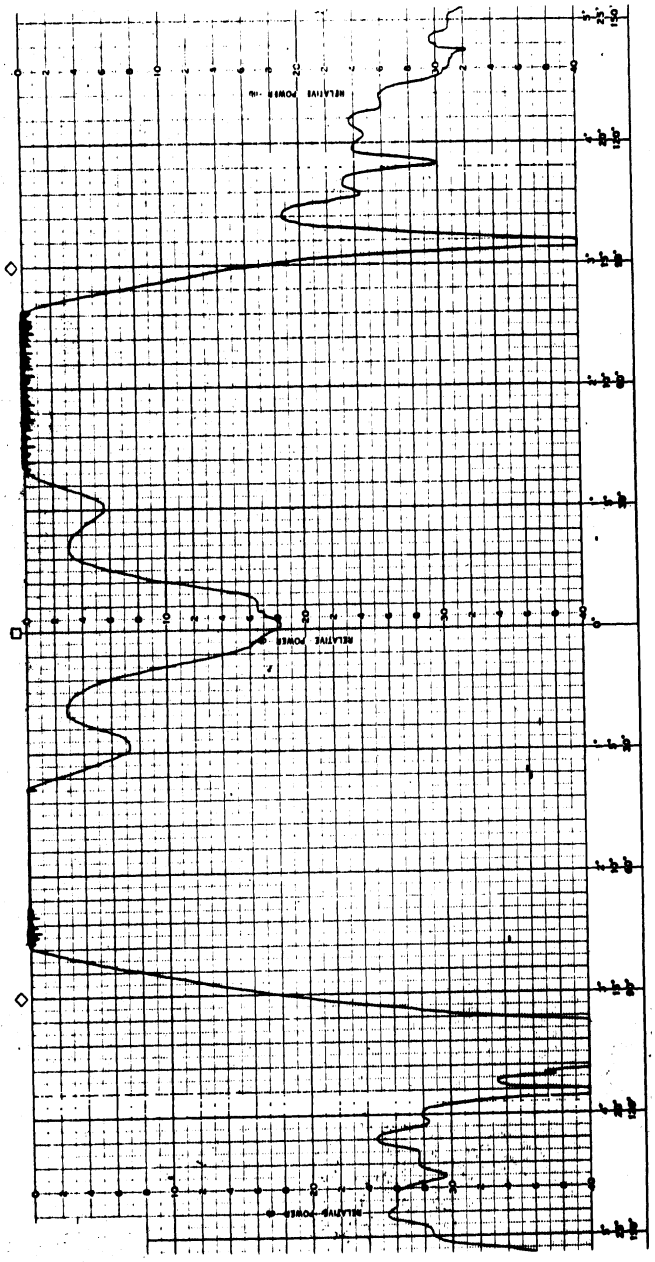

FIG. 4(b): Measured Far Field Elevation Pattern of a Single Parasitic Loop Counterpoise Antenna - Details Near and Below the Horizon. h=4.8", 2A=15', H=22.5", 2B=31.75" and f= 1080 MHz.

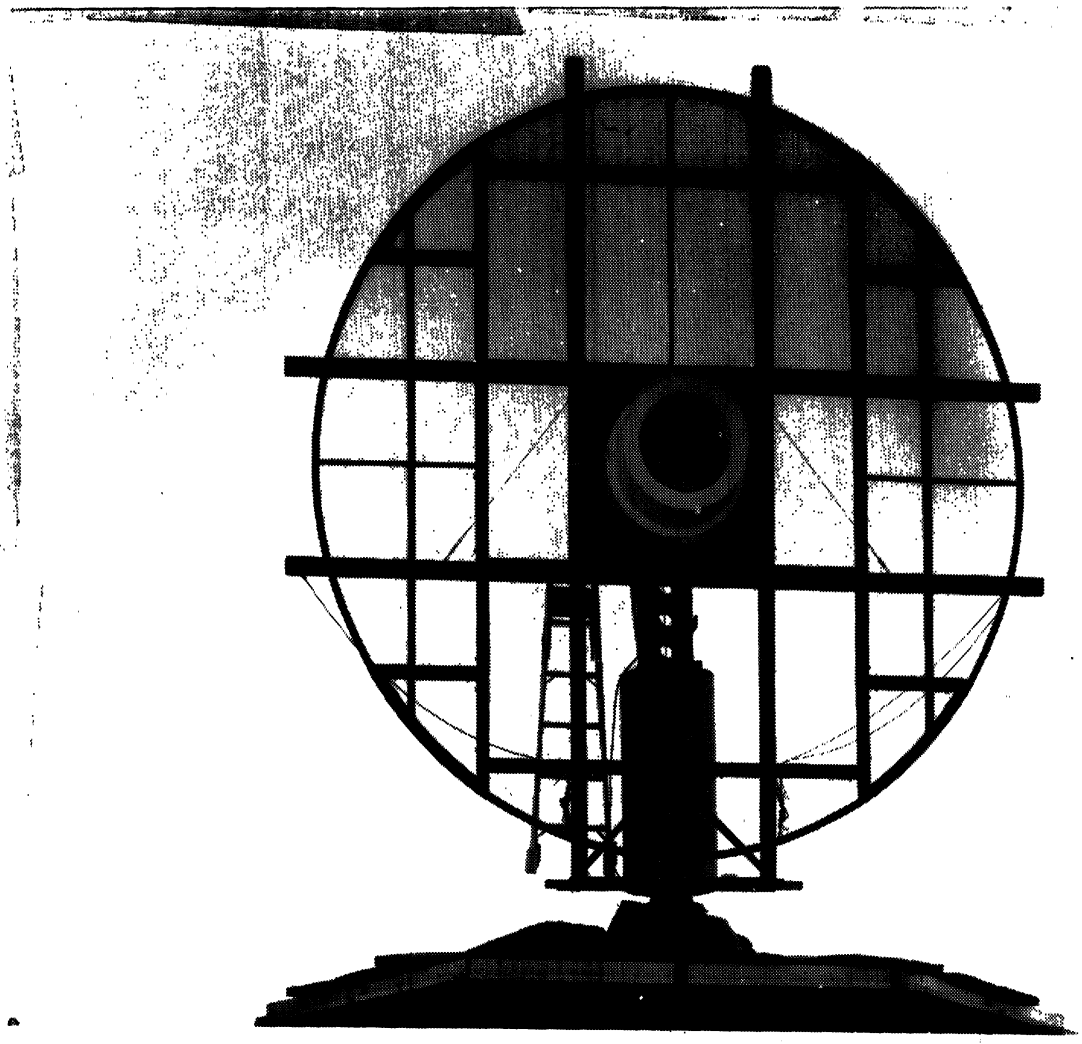

FIG. 5: Photograph of the Double Alford Loop Above the 15' Diameter Counterpoise.

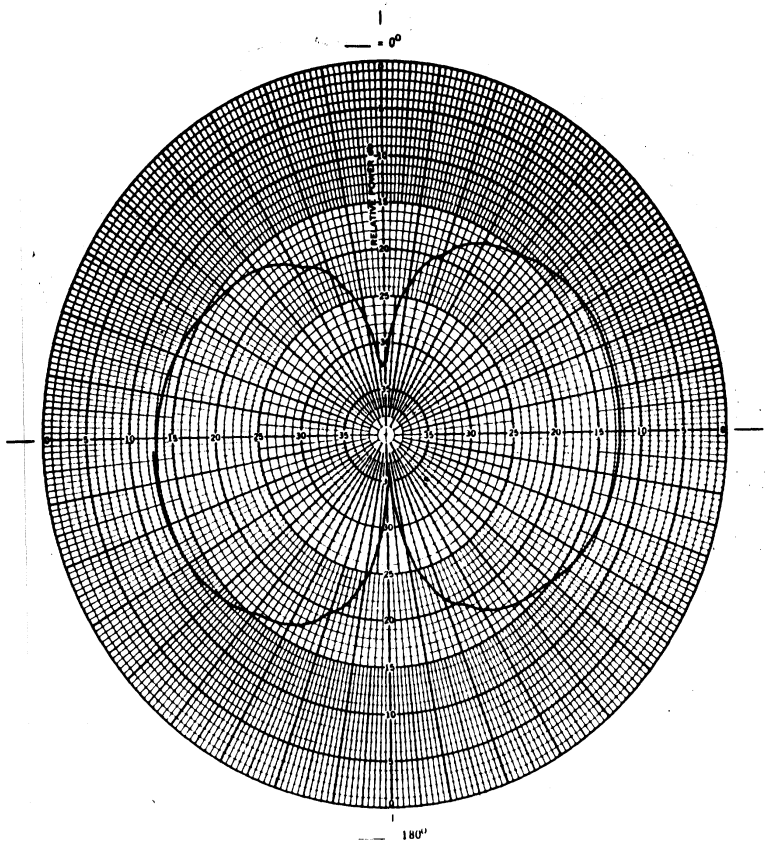

FIG. 6(a): Measured Far Field Patterns of a Double Alford Loop Counterpoise Antenna — Azimuthal Pattern. h=4.8", 2A = 22", f = 1080 MHz.

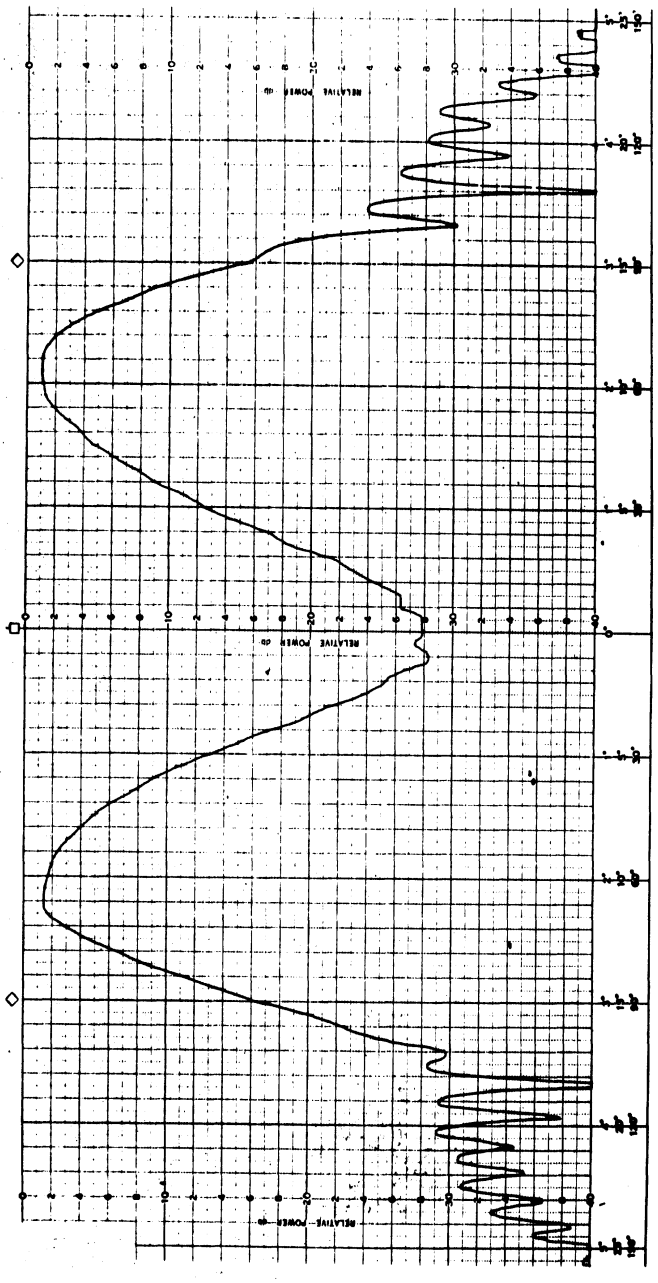

FIG. 6(b): Measured Far Field Patterns of a Double Alford Loop Counterpoise Antenna — Elevation Pattern. h=4.8", 2A = 22", f = 1080 MHz.

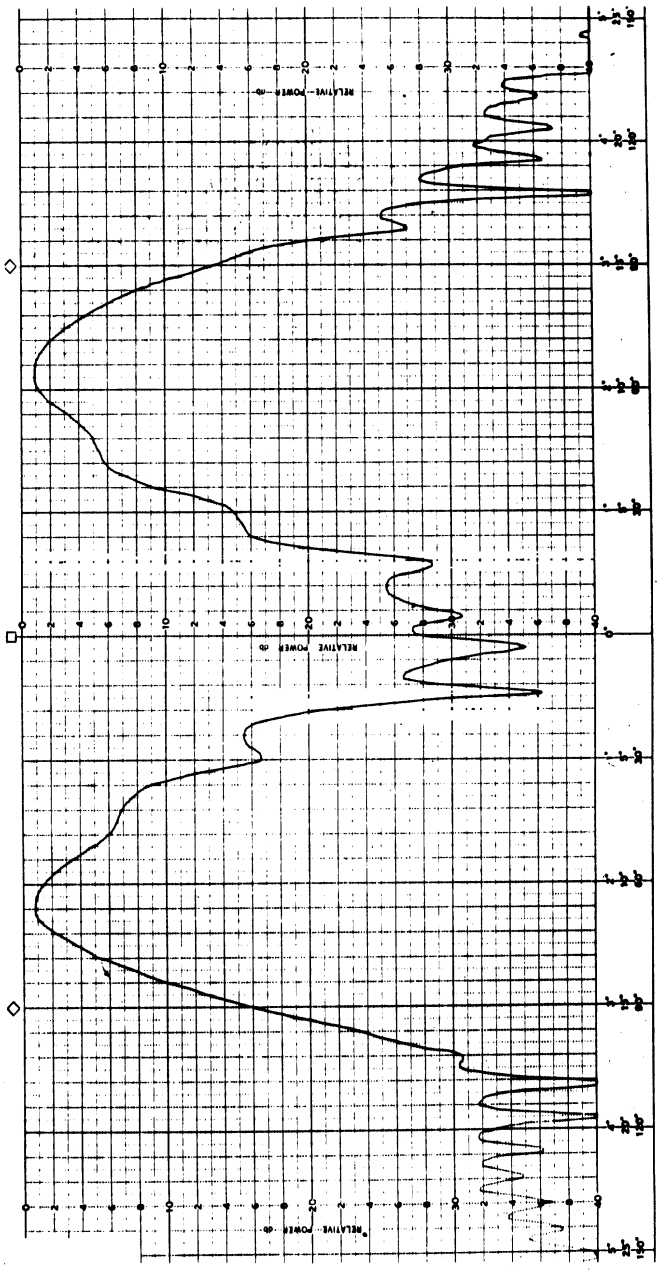

FIG. 7: Measured Far Field Elevation Pattern of a Single Parasitic Loop Counterpoise Antenna with Figure-of-Eight Excitation. h=4.8", 2A=15', H=22.5", 2B = 31.75, W= 1", f = 1080 MHz.